Transcription factor FOXF2 promotes the development and progression of pancreatic cancer by targeting MSI2

BANG-HUA ZHONG, YU-TENG MA, JIAN SUN, JING-TONG TANG and MING DONG

Department of Gastrointestinal Surgery, The First Hospital of China Medical University, Shenyang, Liaoning 110001, P.R. China

Received January 11, 2024; Accepted May 10, 2024

DOI: 10.3892/or.2024.8752

Abstract. Pancreatic cancer (PC) is a malignant tumor possessing high mortality. The role of transcription factor Forkhead Box F2 (FOXF2) in PC remains unverified. The current study investigated the roles of FOXF2 in developing PC *in vitro* and *in vivo*. A xenograft tumor model was constructed with nude mice injected using FOXF2-overexpressing PC cells or FOXF2-silenced PC cells. High FOXF2 expression significantly enhanced the proliferation ability of PC cells *in vitro* and pancreatic tumor growth *in vivo*. The cell cycle analysis indicated that transition of G1-S phase was promoted by FOXF2. The cell cycle-associated proteins cyclin D1, CDK2, phosphorylated (p)-CDK2 and p-RB were upregulated in the FOXF2-overexpressing cells and downregulated in the cells with FOXF2 knockdown. Flow cytometric analysis and Hoechst staining showed that the percentage of apoptotic cells was significantly increased after FOXF2 was silenced. FOXF2 knockdown promoted expression of pro-apoptotic proteins (Bad, Bax and cleaved caspase-3) while suppressing the anti-apoptotic proteins (Bcl-2 and Bcl-xl) at the protein level. FOXF2 improved the migration and invasion of PC cells *in vitro*. Moreover, luciferase and chromatin immunoprecipitation assays revealed that FOXF2 binds to the MSI2 promoter, promoting its transcriptional expression. FOXF2 knockdown inhibited the MSI2 protein translation while enhancing the translation of NUMB protein, suppressing PC development *in vivo*. MSI2 silencing reversed the promotive effect mediated by FOXF2 on cell proliferation. These results demonstrated that FOXF2 is essential in PC progression, and the potential mechanism includes regulating MSI2 transcription.

Introduction

Pancreatic cancer (PC) is an heterogeneous disease with a poor prognosis (1). Globally, PC incidence is associated with various factors such as smoking, family history of chronic pancreatitis, increasing age, male sex and diabetes mellitus. Patients with PC always possess a dismal prognosis. It is estimated that 90% of tumors are diagnosed at an advanced stage after spreading beyond the pancreas, and 50% of tumors have systemic metastasis (2). Hence, understanding the biological and molecular mechanisms of PC and developing a specific target for early PC treatment is essential.

Musashi 2 (MSI2) is one of the RNA-binding proteins originally identified in stem and progenitor cells (3). MSI2 promotes multiple critical biological processes relevant to the development of numerous cancer types, such as PC (4-7). MSI2 induced malignant progression and metastasis of PC and high expression of MSI2 contributed to the migration and invasion of PC cells (4,8,9). As a member of the transcription factor protein group, Forkhead Box F2 (FOXF2) is a mesenchymal transcription factor belonging to the Forkhead Box (FOX) family. FOXF2 functionally promotes cell differentiation and suppresses the mesenchymal transformation of adjacent epithelial cells during embryonic development (10). Evidence has shown that the roles of FOXF2 are complex and controversial across diverse cancers (11). FOXF2 manifests tumor-promoting effects on rhabdomyosarcoma (12). However, FOXF2 inhibits the progression of colorectal (13), cervical (14) and ovarian cancer (15). FOXF2 promotes proliferation, invasion and metastasis in triple-negative breast cancer (16), but inhibits the progression of HER2-positive breast cancer (17). However, the role of FOXF2 in PC has not been elucidated. Based on the bioinformatic prediction (https://jaspar.genereg.net/), the promoter MSI2 region can be bound by the FOXF2 at two binding sites: 5'-tcataataaacaat-3' and 5'-tgataataaacacg-3'. Studies should explore how FOXF2 regulates MSI2 to affect the progression and metastasis of PC. The present study determined the expression level of FOXF2 in clinical PC tissues and investigated its roles in proliferation, apoptosis, invasion and migration of PC cells *in vitro*. The effect of FOXF2 on tumor formation *in vivo* was also evaluated, and the potential regulating mechanism of FOXF2 in PC was illustrated. These results provided detailed insights into the functions of FOXF2 in PC and highlighted that targeting the FOXF2-MSI2 axis might be a promising therapeutic strategy for PC.

Materials and methods

Bioinformatics analyses. The dataset GSE16515 (18) was downloaded from Gene Expression Omnibus (GEO;

Correspondence to: Dr Ming Dong, Department of Gastrointestinal Surgery, The First Hospital of China Medical University, 155 Nanjing North Street, Shenyang, Liaoning 110001, P.R. China
E-mail: dongming@cmu.edu.cn

Key words: forkhead Box F2, Musashi 2, pancreatic cancer

https://www.ncbi.nlm.nih.gov/geo/) and was analyzed through the GEO2R online analysis tool. Differentially expressed genes were screened out with criteria of: log2FoldChange >2.5 and P<0.01. The potential transcription factor was predicted using the HumanTFDB 3.0 database (http://bioinfo.life.hust.edu.cn/HumanTFDB #!). Venn diagram and heatmap analysis were conducted using the R package (version 4.0.2). The JASPAR website (http://jaspar.genereg.net/) was used to predict potential-binding sites between FOXF2 and the promoter of MSI2. The survival prediction and correlation analysis were performed using the Gene Expression Profiling Interactive Analysis (GEPIA) database (http://gepia.cancerpku.cn/). The UALCAN database (http://ualcan.path.uab.edu) showed the expression of FOXF2 in PC tissues.

Reagents and antibodies. The following chemical reagents were used in the present study: BCA assay kit (cat. no. P0009; Beyotime Institute of Biotechnology), Cell Counting Kit-8 (CCK-8; cat. no. C0037; Beyotime Institute of Biotechnology), Hoechst staining kit (cat. no. C0003; Beyotime Institute of Biotechnology), ECL detection kit (BIOSS), Lipo3000 kit (cat. no. L3000015; Invitrogen; Thermo Fisher Scientific, Inc.), 5-ethynyl-20-deoxyuridine (EdU) assay kit (cat. no. KGA335; Nanjing KeyGen Biotech Co., Ltd.), Annexin V-FITC/PI dual-staining kit (cat. no. KGA108; Nanjing KeyGen Biotech Co., Ltd.), Cell Cycle Detection Kit (cat. no. C1052; Beyotime Institute of Biotechnology), Dual Luciferase Reporter Gene Assay Kit (cat. no. KGAF040; Nanjing KeyGen Biotech Co., Ltd.) and chromatin immunoprecipitation (ChIP) Assay Kit (cat. no. P2078; Beyotime Institute of Biotechnology).

The following commercially primary antibodies were used: anti-Ki-67 (1:50; cat. no. AF0198; Affinity Biosciences), anti-FOXF2 (1:500; cat. no. D260341; Sangon Biotech Co., Ltd.), anti-NUMB (1:200; cat. no. D122795; Sangon Biotech Co., Ltd.), anti-MSI2 (1:200; cat. no. D198948; Sangon Biotech Co., Ltd.), anti-cyclin D1 (1:1,000; cat. no. bs-20596R; BIOSS), anti-CDK2 (1:1,000; cat. no. bs-10726R; BIOSS), anti-p-CDK2 (1:1,000; cat. no. bs-3483R; BIOSS), anti-p-RB (1:2,000; cat. no. bsm-52197R; BIOSS), anti-Cleaved caspase-3 (1:500; cat. no. bs-20364R; BIOSS), anti-Bax (1:500; cat. no. bs-0127R; BIOSS), anti-Bad (1:500; cat. no. bs-0892R; BIOSS), anti-Bcl-xl (1:1,000; cat. no. bsm-52024R; BIOSS), anti-Bcl-2 (1:1,000; cat. no. bsm-52304R; BIOSS) and anti-β-actin (1:500; cat. no. bs-0061R; BIOSS). The secondary antibodies included: Goat anti-rabbit IgG conjugated with horseradish peroxidase (IgG-HRP; 1:500; cat. no. 31460; Thermo Fisher Scientific, Inc.), rabbit anti-mouse IgG-HRP (1:10,000; cat. no. bs-0377R-HRP; BIOSS) and goat anti-rabbit IgG-HRP (1:10,000; cat. no. bs-40295G-HRP; BIOSS).

Human tissues. Fresh samples of PC and adjacent normal tissue (n=29), and clinical paraffin samples from 78 cases of patients with PC were obtained in the First Hospital of China Medical University (Shenyang, China) from September 8, 2021 to April 7, 2022. The expression of FOXF2 and MSI2 in cancer and adjacent normal tissue was detected by reverse transcription-quantitative PCR (RT-qPCR). Clinical paraffin samples were used for immunohistochemical (IHC) staining of FOXF2, followed by analyzing the association between FOXF2 expression and clinicopathological characteristics of patients with PC. The characteristics of the cases were collected from the hospital medical records. Pathological staging was carried out based on the eighth edition of with American Joint Committee on Cancer. All experiments using human tissue were approved [approval no. (2021) 113] by the Medical Science Research Ethics Committee of The First Affiliated Hospital of China Medical University (Shenyang, China). Written informed consent for the collection of tissue samples was provided by all patients.

Cell lines and culture. The human PC cell line AsPC-1 (Procell Life Science & Technology Co., Ltd.) was maintained in RPMI-1640 medium (Beijing Solarbio Science & Technology Co., Ltd.) containing 10% fetal bovine serum (FBS; Zhejiang Tianhang Biotechnology Co., Ltd.). PANC-1 (iCell; http://m.icellbioscience.com/) was maintained in DMEM medium (Wuhan Servicebio Technology Co., Ltd.) containing 15% FBS. These PC cell lines were all cultured at 37˚C with 5% CO_2.

Plasmid construction and RNA interference. Small interfering RNA (siRNA) targeting FOXF2 (siFOXF2), MSI2 (siMSI2) and untargeted interfering RNA (siNC) were synthesized by JTSBIO Co., Ltd. For establishment of stable cell line with FOXF2 knockdown, the (shFOXF2) was inserted to pRNA-H1.1 plasmid. The untargeted shRNA (shNC) served as negative control. The construction of plasmid of shFOXF2 was completed by Anhui General Biotechnology Co., Ltd. pcDNA3.1 was used for FOXF2-overexpressing plasmid (FOXF2) construction and empty vector was used as negative control (vector). FOXF2-overexpressing plasmids were purchased form Zhejiang Tianyuan Biotechnology Co., Ltd. Transfections were performed in 6-well plates when the cells were ~70% confluent. For each well, a mixture with 125 μl Opti-MEM, 2.5 μg plasmids or 75 pmol siRNA, and 5 μl Lipofectamine 3000 reagent was prepared. This mixture was added to a solution containing 7.5 μl Lipofectamine 3000 and 125 μl Opti-MEM. After a 15-min incubation, the solution was added drop-wise to the cells for 48 or 24 h in a 37˚C incubator. Transfection was carried out according to the Lipo3000 kit manufacturer's instructions (cat. no. L3000015; Invitrogen; Thermo Fisher Scientific, Inc.). The sequences of all siRNAs used in the present study were as follows: siFOXF2-1, 5'-GCUUCAUCAAGCUGCCUAATT-3'; siFOXF2-2, 5'-GCGAGUUCAUGUUCGAGGATT-3'; siMSI2, 5'-AGUGGAAGAUGUAAAGCAATT-3'; and siNC, 5'-UUCUCCGAACGUGUCACGUTT-3'.

Western blotting (WB). The total protein was extracted with radio immunoprecipitation assay (RIPA) lysis buffer (cat. no. P0013B; Beyotime Institute of Biotechnology,) containing 1% PMSF (cat. no. ST506; Beyotime Institute of Biotechnology), fully lysed for 5 min on ice, and then centrifuged at 10,000 x g for 3 min at 4˚C. The concentration of total protein was detected by BCA assay kit. Next, equal volumes of protein lysate (15 μl, 15-30 μg protein) were separated by 8-14% SDS-PAGE and electrically transferred into polyvinylidene difluoride membranes (Thermo Fisher Scientific, Inc.). The membranes were then blocked with 5% BSA (Biosharp Life Sciences) for 60 min at room temperature and incubated

with primary antibodies overnight at 4˚C. Subsequently, the membranes were incubated with secondary antibodies at 37˚C for 40 min. Immunoreactive protein bands were visualized with an ECL detection kit (cat. no. C05-07004; BIOSS) and the images were analyzed by gel image processing system.

RT-qPCR. RT-qPCR assay was carried out with SYBR Green (cat. no. SY1020; Beijing Solarbio Science & Technology Co., Ltd.) as previously described with slight modifications (8). In brief, extracted RNA was reverse transcribed to cDNA by using a kit (cat. no. D7160L; Beyotime Institute of Biotechnology,) according to the manufacturer's instructions, and then it was analyzed using a real time fluorescence quantitative PCR instrument (Bioneer Corporation). The thermocycling conditions for qPCR were as follows: 94˚C for 5 min, 94˚C for 15 sec, 60˚C for 25 sec and 72˚C for 30 sec with 40 cycles, followed by 72˚C for 5.5 min, 40˚C for 2.5 min, melting 60˚C to 94˚C, every 1.0˚C for 1 sec and 25˚C for 1-2 min. The data were calculated using the $2^{-\Delta\Delta Cq}$ method (19) and presented as relative expression fold change. The value in controls was arbitrarily set as 1. The primers were synthesized by Sangon Biotech Co., Ltd. and sequences were as follows: FOXF2 forward, 5'-CAGGGC TGGAAGAACTCGG-3' and reverse, 5'-CGGTGGTACATG GGCTTGA-3'; MSI2 forward, 5'-CCCAGCAAGTGTAGA TAAAG-3' and reverse, 5'-GTGACAAAGCCAAACCC-3'; and β-actin forward, 5'-CACTGTGCCCATCTACGAGG-3' and reverse, 5'-TAATGTCACGCACGATTTCC-3'.

CCK-8 assay. The cell proliferation was measured by using CCK-8 assay kit according to the manufacturer's instructions. After 24 h transfection, cells ($4x10^3$/well) were seeded in 96-well plates with five replicates and incubated at 37˚C with 5% CO_2 for 0, 24, 48 and 72 h. The co-transfected cells were incubated at same conditions for 48 h. Each well was added with 10 μl CCK-8 solution and incubated at 37˚C for 48 h. The results were determined by the optical density values of absorbance at 450 nm.

EdU staining assay. According to protocol of the EdU assay kit, cells ($5x10^4$/well) were cultured with preheated EdU solution in 24-well plates at 37˚C for 2 h. Next, the cells were fixed with 4% paraformaldehyde for 15 min and then incubated with 0.5% Triton X-100 at room temperature for 20 min. After being dyed with 2-(4-Amidinophenyl)-6-indolecarbamidine dihydrochloride (DAPI, 1 μg/ml) for 5 min, the stained cells were observed under a fluorescence microscope (Olympus Corporation).

Cell cycle analysis. Cells were washed with cold phosphate-buffered saline and fixed in 75% ethanol overnight at 4˚C. Next, the cells were dyed using 25 μl propidium iodide (PI) solution and incubated in darkness for 30 min with 10 μl RNase A at 37˚C, followed by detection using NovoCyte flow cytometer (ACEA Bioscience, Inc.) and analysis by a NovoExpress software (NovoExpress 1.4.1; Agilent Technologies, Inc.).

Cell apoptosis analysis. Cell apoptosis was analyzed by using the Annexin V-FITC/PI dual-staining kits according to the manufacturer's protocol and it was finally detected using NovoCyte flow cytometer.

Hoechst staining. The transfected cells ($1x10^5$/well) were seeded in 12-well plates, incubated at 37˚C with 5% CO_2 for 48 h, and stained with Hoechst staining solution for 5 min. The apoptotic cells were observed under an inverted fluorescent microscope (Olympus Corporation).

Wound healing assay. Cell migration was detected by wound healing assay. Briefly, the confluent cells were serum-starved and treated with 1 μg/ml Mitomycin C (cat. no. M0503; Sigma-Aldrich; Merck KGaA) at 37˚C for 1 h. Subsequently, cells were scratched using a pipette tip and cultured at 37˚C with 5% CO_2 for 24 h. The distance migrated by the cells into the wound was measured.

Transwell assay. The invasive ability of cells was determined by Matrigel-coated Transwell inserts (0.4μm) (LABSELECT, http://www.labselect.cn/index/product/details/language/cn/product_id/149.html). Matrigel was precoated on the inserts at 37˚C for 2 h in the 24-well plate. After 24 h transfection, the cell suspension ($5x10^4$) was seeded into the upper chamber of this system with no medium. The lower chamber was added RPMI-1640 or DMEM medium containing 10% FBS. After incubation for 24 h, they were fixed by 4% paraformaldehyde at room temperature (25˚C) and stained with 0.4% crystal violet. The number of invasive cells was counted under a light microscope in five randomly selected fields.

Luciferase reporter assay. A total of two potential binding sites were predicted followed by designing two reporter plasmids to explore how FOXF2 binds to the MSI2 promoter regions: pGL3-MSI2 promoter (-1987/+11) and pGL3-MSI2 promoter (-1824/+11). The pRL-TK and pGL3-basic plasmids were both from Fenghui Biotechnology Co., Ltd. Luciferase reporter plasmid constructions were synthesized by Anhui General Biotechnology Co., Ltd. For the luciferase reporter assay, 293 cells (purchased frOm iCell company) were co-transfected with the reporter plasmids and the plasmid of FOXF2 or vector by using a Lipo3000 kit. After being cultured for 48 h, luciferase activity was measured by the dual luciferase reporter gene assay kit according to the manufacturer's instructions. The ratio of firefly luciferase intensity/*Renilla* luciferase intensity indicated a relative luciferase activity.

ChIP-PCR assay. ChIP-PCR assay was performed using a ChIP Assay Kit. Briefly, the collected cells were lysed in SDS lysis buffer and then sonicated to obtain DNA fragments. Next, protein-DNA complexes were respectively precipitated by IgG or FOXF2 antibody (1:100), followed by complex elution. The immunoprecipitated DNA was amplified with 2X Taq PCR MasterMix (cat. no. PC1150; Beijing Solarbio Science & Technology Co., Ltd.). The thermocycling conditions for qPCR were as follows: 95˚C for 5 min, 95˚C for 20 sec, 55˚C for 20 sec and 72˚C for 30 sec with 40 cycles, followed by 72˚C for 2 min, 25˚C for 5 min. The sequences of a pair primer specific for the MSI2 promoter were as follows: Forward, 5'-CTGTTG TCTGCATTTTG-3' and reverse, 5'-GTCTCCCTGTTCCCT AA-3'). Agarose gel electrophoresis (2.0%; containing gold view nucleic acid dye) was performed on electrophoresis apparatus (Beijing Liuyi Instrument Factory), and the images was

captured by Gel Imaging System (WD-9413B; Beijing Liuyi Biotechnology).

Xenograft tumor model. Male BALB/C nude mice (aged 4 months; weight, 20-25 g) were used to establish xenograft tumor model. Animals were housed in a 12/12-h of light/dark cycle at 22˚C with 45-55% humidity and adaptively provided with free access to water and food. All animal experiments were performed according to the National Institutes of Health Guide for the Care and Use of Laboratory Animals. All animal studies were approved (approval no. KT2021051) by the Laboratory Animal Welfare and Ethics Committee of China Medical University (Shenyang, China). A total of 24 mice were used in the present study. Subcutaneous injection with PC cells ($5x10^6$ cells) resuspended in 200 μl PBS, was used to establish the PC mouse model (20). The nude mice were randomly divided into four groups (6 mice per group) that received subcutaneous injection (at dorsal region) of vector-transfected AsPC-1 cells, FOXF2-transfected AsPC-1 cells, shNC-transfected PANC-1 cells and shFOXF2-transfected PANC-1 cells, respectively. From day 7 after injection, tumor volume was measured every three days. The tumor volume was calculated as follows: Volume=0.5 x long diameter x short diameter^2. Mice bearing subcutaneous tumors were euthanized upon reaching humane endpoints of tumor size. A tumor diameter exceeding 17 mm was considered as humane endpoint. Mice were euthanized by carbon dioxide asphyxiation (40% vol/min flow rate in the chamber). Death was confirmed when the mice were immobile, ceased breathing and with dilated pupils. The mice were observed for a further 5 min to confirm their death. The tumor body was removed for measurement of tumor weight and pathological assessment.

Hematoxylin and eosin (H&E) staining and IHC staining. H&E staining was performed according to standard procedures and the results of staining were observed under a light microscope. For IHC staining, the tissues were fixed in 10% formalin overnight at 25˚C, and embedded in paraffin. Next, 5-μm paraffin sections were deparaffinized by xylene and rehydrated in 95, 85 and 75% ethanol, each for 3 min. Next, the sections were subjected to antigen-retrieval with citrate buffer at 95˚C for 10 min. After endogenous peroxidase removal by 3% H_2O_2, the sections were blocked with 1% BSA for 15 min at room temperature and incubated overnight with anti-Ki-67 (1:50) or anti-FOXF2 (1:50) at 4˚C. A secondary antibody goat anti-rabbit IgG-HRP (1:500) was utilized to incubate these sections at 37˚C for 1 h. The sections were visualized by diaminobenzidine (DAB) solution (Maxim Biomedical, Inc.) and finally observed under a light microscope. Quantitative evaluation of the IHC staining was performed based on the staining density and stained proportion. The score of stained proportion was based on a scale of 0-3 point (0, ≤10%; 1, 11-25%; 2, 26-50%; and 3, >51%). The staining density was scored as 0 points, weak staining as 1 point, intermediate staining as 2 points, and strong staining as 3 points. The IHC score was calculated as percentage score x intensity score. FOXF2 staining in tissues was classified into two categories (low and high expression): The specimens with an IHC score 0-4 were defined as the low FOXF2 expression group and specimens with an IHC score >4 as the high FOXF2 expression group. Ki-67 index was calculated as the percentage of Ki-67-positive cells. The specimens were graded by the Ki-67 index according to the WHO 2010 classification (G1: Ki-67 Index, <3%; G2: Ki-67 Index, 3-20%; and G3 NET/NEC: Ki-67 Index, >20%) (21).

Statistical analysis. All the experiments were performed with at least three independent replicates and the data were expressed as the mean ± SD. Statistical analyses were performed with GraphPad Prism 8 software (GraphPad Software Inc.; Dotmatics). Pearson's correlation analysis was performed for the expression of MSI2 and FOXF2. Two-tailed unpaired t-test was used to analyze two groups. One-way ANOVA followed by a Tukey's test or two-way ANOVA followed by a Sidak post hoc test was performed for comparing more than two groups. The Chi-square test and Fisher's exact test were used to analyze the association between the expression level of FOXF2 and pathological characteristics in pancreatic cancer. $P<0.05$ was considered to indicate a statistically significant difference.

Results

Expression of FOXF2 in PC. MSI2 is a tumor-promoting factor in PC and a previous study by the authors elucidated several downstream regulatory mechanisms of MSI2 in PC development (4). The potential transcription factors that were predicted to be bound with MSI2 were obtained and the upstream regulatory mechanism of MSI2 was explored. Moreover, the differentially expressed genes form PC the dataset GSE16515 were also screened with criteria of: $|\log2FoldChange| > 2.5$ and $P<0.01$. A total of 541 differentially expressed genes were selected and 291 potential transcription factors were predicted. Based on Venn intersection analysis, 9 genes were identified (Fig. 1A); 2 genes downregulated and 7 genes upregulated. Among them, FOXF2 was the most markedly upregulated gene (Fig. 1B). However, its roles in PC have not been explored. From GEPIA database, it was also found that the expression level of FOXF2 was significantly higher in PC tissue than normal tissue ($P<0.05$) and high expression of FOXF2 was associated with worse overall survival in patients with PC (Fig. 1C). Furthermore, the correlation analysis indicated that FOXF2 expression was positively related with MSI2 expression ($R=0.8$, $P<0.001$) (Fig. 1D). Subsequently, the expression of FOXF2 and MSI2 was detected in 29 pairs of PC tissues and adjacent normal tissues by RT-qPCR. As shown in Fig. 1E, both the expression level of FOXF2 and MSI2 were higher in PC tissues than in adjacent normal tissues ($P<0.01$). Consistent with the result from GEPIA database, FOXF2 expression was positively correlative with MSI2 expression in these paired PC tissues ($R=0.8$, $P<0.001$) (Fig. 1F). Additionally, clinical samples were analyzed to explore the relationship between FOXF2 expression and clinicopathological characteristics including age, sex, TNM staging and differentiation. The representative IHC images of low or high expression level of FOXF2 in clinical PC tissues were shown in Fig. 1G. Among of 78 specimens, 36 cases were identified as high level of FOXF2 and 42 cases as low level of FOXF2. It was found that FOXF2 expression was significantly associated with T stage of PC and high expression level of FOXF2 was associated with an advanced T stage (larger tumor) (Table I), suggesting that FOXF2 might contribute to the progression of PC. Besides,

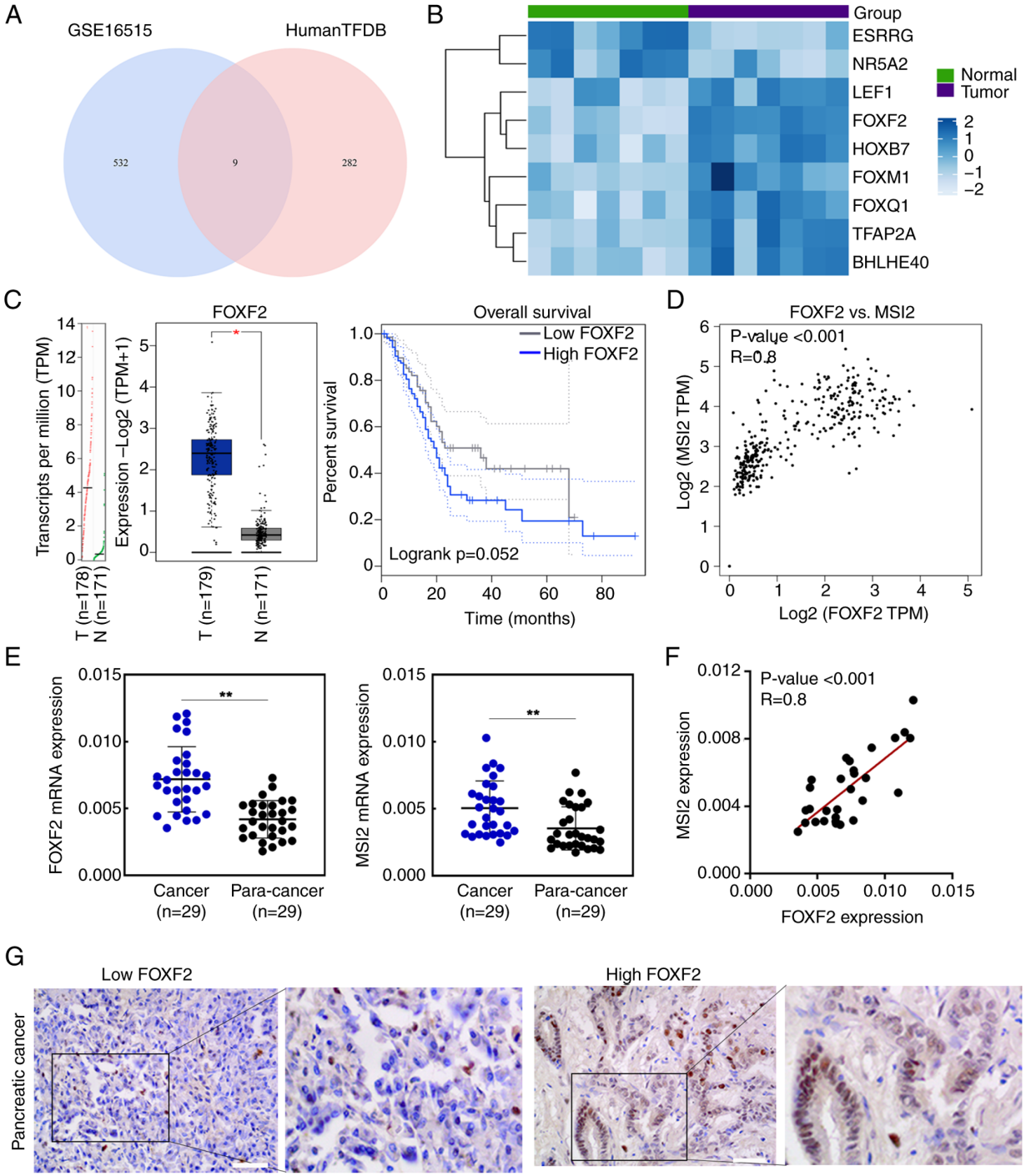

Figure 1. Expression of FOXF2 and MSI2 in PC. (A) Venn diagrams characterize the overlaps between differentially expressed genes in GSE16515 and predicted transcriptional factor from Human TFDB database. (B) Heatmap showed the expression of 9 intersection genes in PC. (C) FOXF2 expression in PC (GEPIA). (D) The correlation between FOXF2 and MSI2 displayed by scatter plot (GEPIA). (E) Reverse transcription-quantitative PCR assay determined the expression of FOXF2 and MSI2 in PC and adjacent normal tissues. (F) The correlation between FOXF2 and MSI2 was validated. (G) The representative pictures from immunohistochemical staining for FOXF2 of tumors. *P<0.05 and **P<0.01. FOXF2, forkhead Box F2; MSI2, Musashi 2; PC, pancreatic cancer; GEPIA, Gene Expression Profiling Interactive Analysis.

patients with high FOXF2 expression tended to have a higher Ki-67 index. No significant association was observed between FOXF2 expression and differentiation in the clinical samples collected. The UALCAN database indicated that FOXF2 is highly expressed in the PC tissue with grade 3 compared with normal samples (Fig. S1), but most of the collected specimens were moderately differentiated, which is responsible for this absence of association in the present study.

FOXF2 accelerates PC cell proliferation. FOXF2 was efficiently silenced or overexpressed within AsPC-1 cells or PANC-1 cells at mRNA and protein levels after transfection (P<0.01) (Fig. S2A and B). CCK-8 assay revealed that the proliferation of the cells with FOXF2 overexpression was significantly higher than in vector-transfected cells (P<0.01), and FOXF2 knockdown significantly decreased proliferation of PANC-1 cells (P<0.05) (Fig. 2A). Consistently, the EdU staining

Table I. Association between the expression level of FOXF2 and pathological characteristics in pancreatic cancer.

Clinicopathological characteristics	Number of cases	Expression level of FOXF2		P-value
		High (36)	Low (42)	
Age, years				0.082
<60	32	11	21	
≥60	46	25	21	
Sex				0.064
Male	41	23	18	
Female	37	13	24	
T stage				0.0029
T1 + T2	68	27	41	
T3 + T4	10	9	1	
N stage				0.738
N0	60	29	31	
N1	16	6	10	
N2	2	1	1	
American Joint Committee on Cancer TNM staging				0.892
I/II	75	34	41	
III	3	2	1	
Differentiation				0.066
High	12	9	3	
Middle	53	23	30	
Low	13	4	9	
Ki-67 index				0.0003
G1	13	0	13	
G2	12	4	8	
G3	53	32	21	

FOXF2, forkhead Box F2.

results presented that FOXF2 overexpression augmented proliferation and FOXF2 knockdown decreased it (Fig. 2B). The cell cycle analysis suggested that the proportion of cells in G1/G2 phase declined and the proportion in S phase was increased after FOXF2 overexpression (P<0.01). Compared with the siNC-transfected cells, the percentage of cells in G1/G2 phase was increased and the percentage in S phase was decreased in the FOXF2-silenced cells (P<0.01) (Fig. 2C and D). It was indicated that FOXF2 contributed to the G1-S phase transition in PC cells. Cyclin D1, CDK2, p-CDK2 and p-RB are major cell cycle regulatory proteins and primarily involve G1/S phase transition (22). The expression level of these proteins was increased after FOXF2 overexpression while it was decreased in the FOXF2-slienced cells (Fig. 2E). The aforementioned results indicated that FOXF2 promotes the proliferation of PC cells by accelerating G1-S phase transition.

FOXF2 knockdown induces apoptosis of PC cells. Flow cytometric analysis showed that cell apoptosis was increased after FOXF2 was silenced (P<0.01) (Fig. 3A and B). Consistently, Hoechst staining manifested that FOXF2 knockdown increased the number of apoptotic cells (Fig. 3C). Besides, the expression of anti-apoptotic proteins (Bcl-2 and Bcl-xl) was downregulated in the FOXF2-silenced cells. The expression of pro-apoptotic proteins (Bad, Bax and Cleaved capase-3) was upregulated in the cells with FOXF2 knockdown (Fig. 3D). Collectively, it was indicated that knockdown of FOXF2 induces apoptosis of PC cells.

FOXF2 promotes migration and invasion of PC cells. Cell migration was assessed using the wound healing assay. The wound closure area of FOXF2-overexpresseing cells was less wide than that of vector-transfected cells, and the wound closure area of FOXF2-silenced cells was smaller than that of siNC-transfected cells (Fig. 4A). Transwell assay was performed for cell invasion. As shown in Fig. 4B and C, FOXF2 overexpression increased the number of invasive cells and FOXF2 knockdown decreased it. These results suggested that FOXF2 may act as a tumor-progressing factor to enhance the migration and invasion of PC cells.

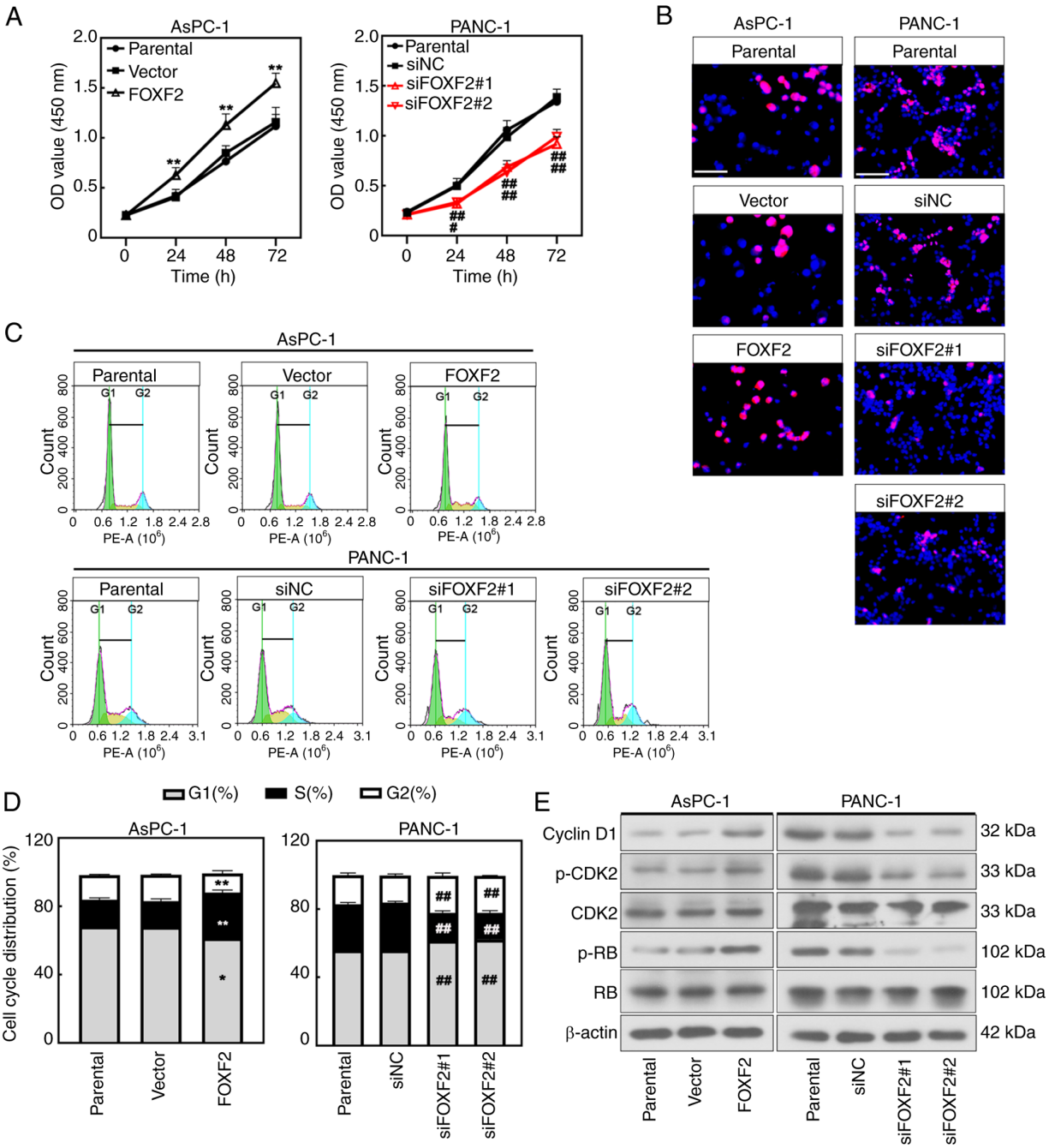

Figure 2. FOXF2 accelerates PC cell proliferation. PC cell line AsPC-1 was transfected with FOXF2 overexpression plasmid or empty vector. PANC-1 cells were transfected with FOXF2 siRNA (siFOXF2) or siNC. (A) Cell proliferation was examined at 24, 48 and 72 h. (B) EdU staining detected cell proliferation ability. (C and D) Flow cytometric analysis of cell cycle distribution. (E) Western blot detection of the cell cycle-related proteins cyclin D1, CDK2, p-CDK2 and p-RB. β-actin served as a loading control. Data are presented as the mean ± SD of at least three independent measurements (n=3). *P<0.05 and **P<0.01 vs. vector; $^{\#}$P<0.05 and $^{\#\#}$P<0.01 vs. siNC. FOXF2, forkhead Box F2; PC, pancreatic cancer; siRNA, small interfering RNA; NC, negative control; p-, phosphorylated.

FOXF2 promotes malignant behavior of PC cells possibly by regulating MSI2. Analysis through the bioinformatics prediction website (https://jaspar.genereg.net/) predicted that FOXF2 could be a potential regulator of MSI-2. A total of two luciferase reporter plasmids with the fragment of MSI2 promotor region were constructed to explore how FOXF2 regulates MIS2 in PC cells. Luciferase assays revealed that FOXF2 bound to the MSI2 promoter and FOXF2 overexpression significantly enhanced the luciferase activity of MSI2 reporter plasmid (P<0.01) (Fig. 5A). Moreover, this result was validated within PC cells by ChIP assay (Fig. 5B). The mRNA expression of MSI2 was increased in the FOXF2-overexpressing cells and decreased in the FOXF2-silenced cells (P<0.01) (Fig. 5C). MSI2 protein expression showed similar trends as mRNA level (Fig. 5D). NUMB protein, a tumor suppressor that is negatively regulated by MSI2, was markedly decreased in the cells with FOXF2 overexpression and increased in the cells with FOXF2 knockdown (Fig. 5D). AsPC-1 cells were co-transfected with using FOXF2-overexpressing plasmid and interference sequence siMSI2 to investigate the regulatory

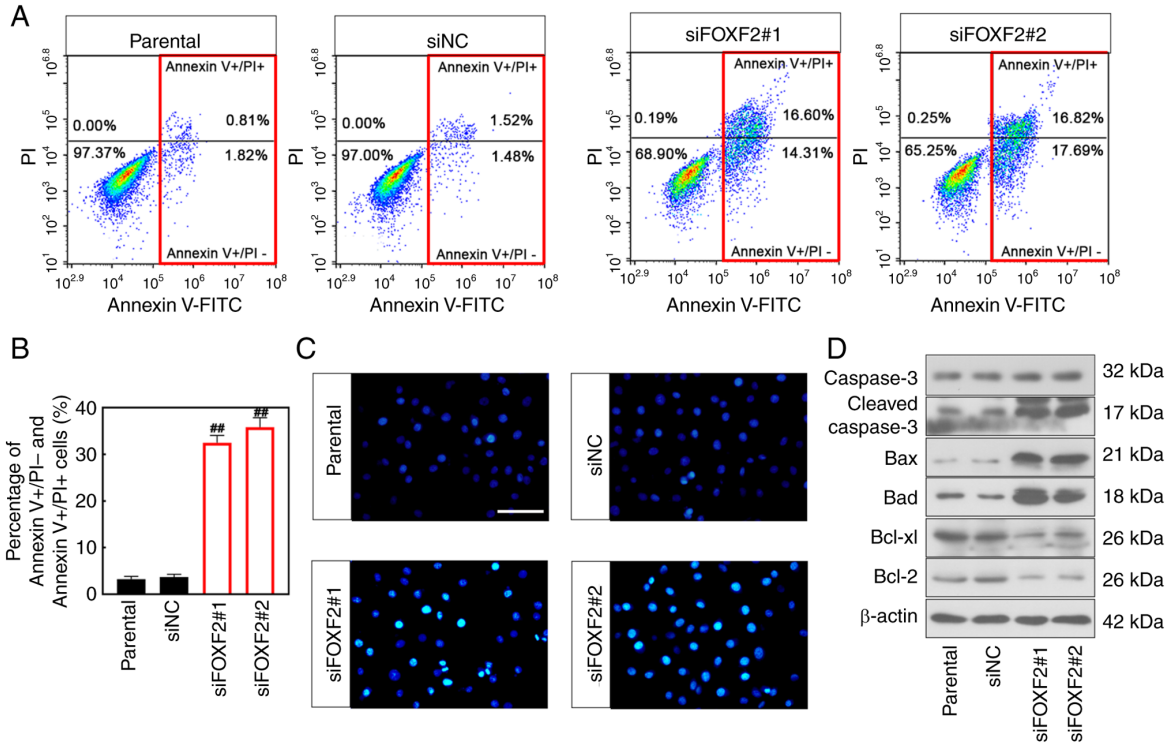

Figure 3. FOXF2 knockdown induces apoptosis of pancreatic cancer cells. (A and B) Flow cytometric analysis showed apoptosis of PANC-1 cells after transfection. (C) Hoechst staining of apoptosis. Magnification, x200; scale bars, 100 μm. (D) Western blot assay was performed to detect the expression of apoptosis-related proteins Cleaved caspase-3, Bax, Bad, Bcl-xl and Bcl-2. Data are expressed as the mean ± SD of at least three independent measurements (n=3). $^{\#\#}$P<0.01 vs. siNC. FOXF2, forkhead Box F2; si-, small interfering; NC, negative control.

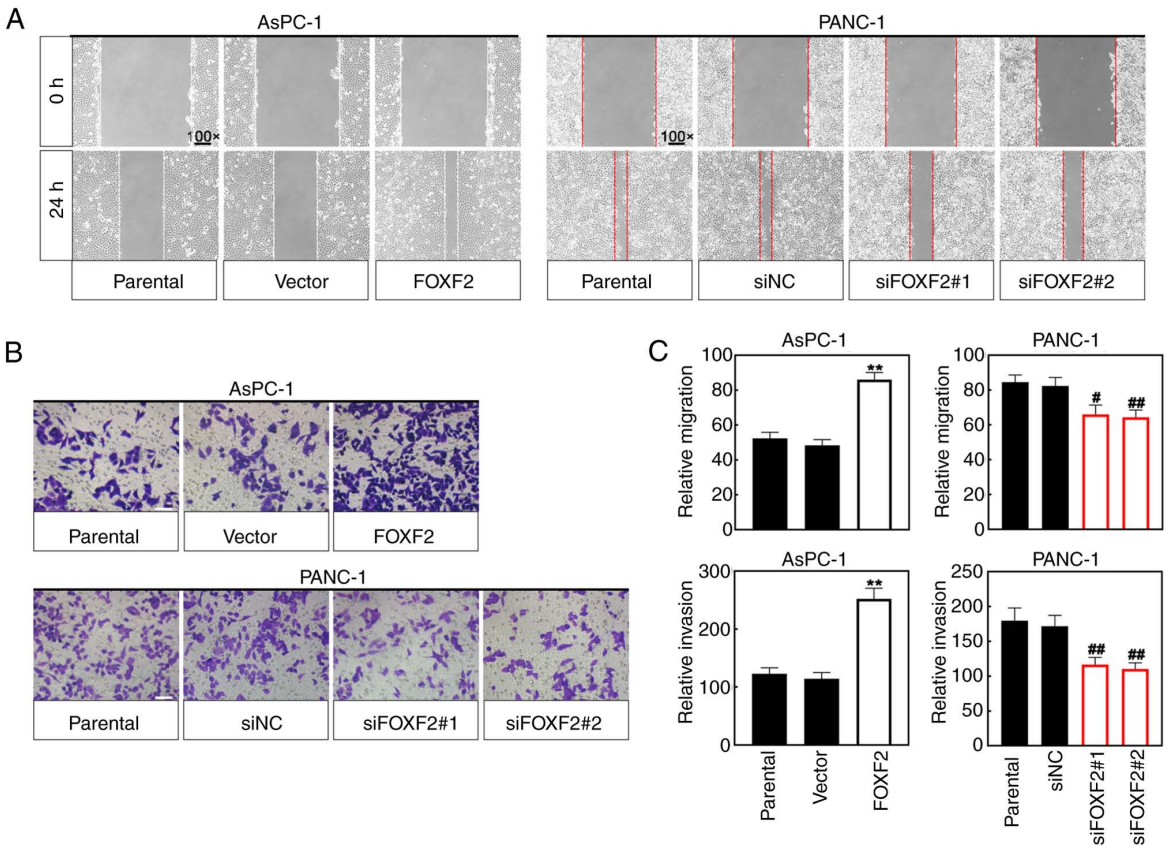

Figure 4. FOXF2 promotes migration and invasion of pancreatic cancer cells. (A) Wound healing assay was used to show the migratory ability of AsPC-1 and PANC-1 cells. (B) Cell invasion ability was detected by Transwell assay. (C) Quantified results of wound healing and Transwell assays. Data are indicated as the mean ± SD of at least three independent experiments (n=3). **P<0.01 vs. vector; $^{\#}$P<0.05 and $^{\#\#}$P<0.01 vs. siNC. FOXF2, forkhead Box F2; si-, small interfering; NC, negative control.

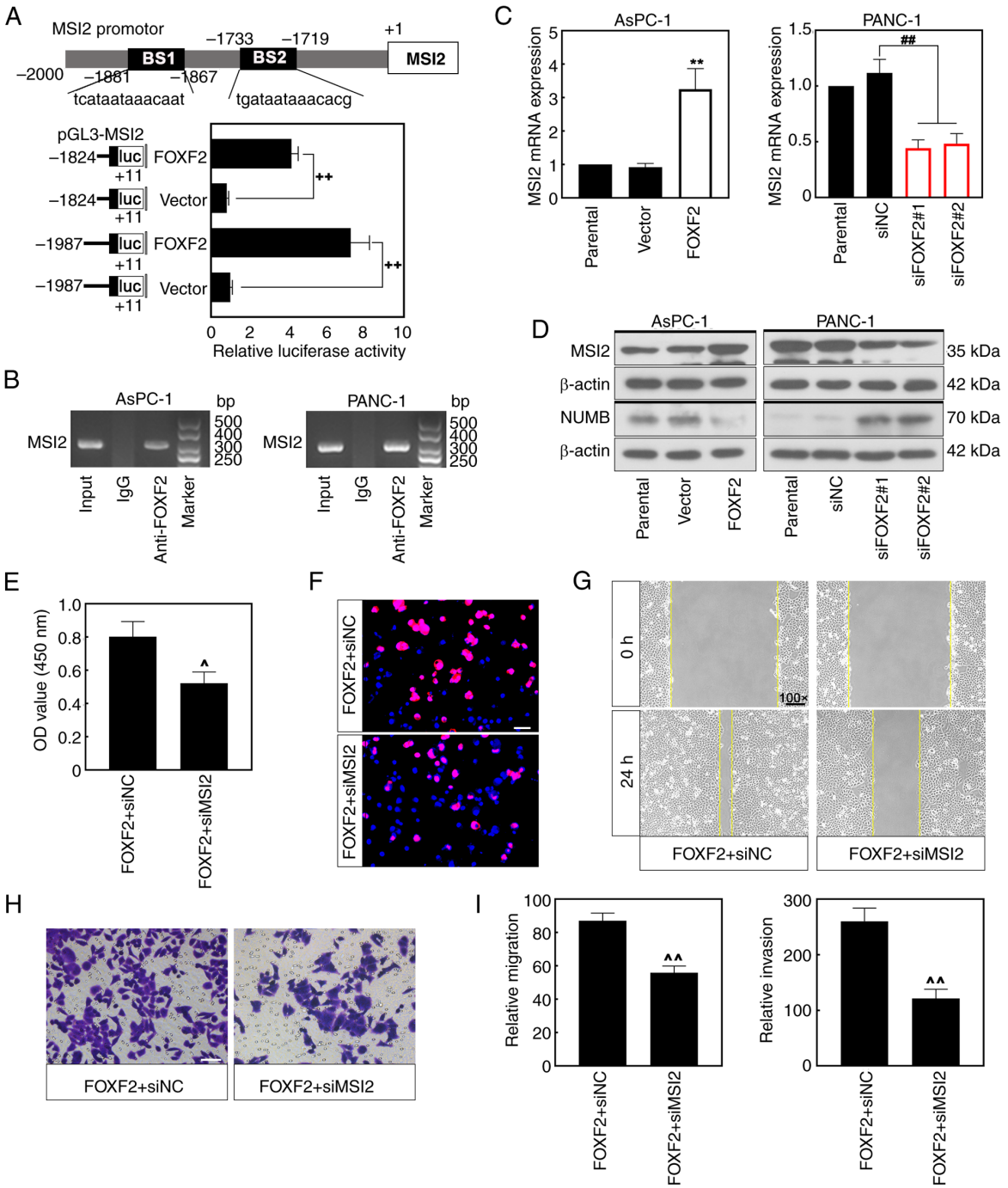

Figure 5. FOXF2 promotes malignant behavior of PC cells possibly by regulating MSI2. (A) 293 cells were transfected with indicated MSI2 promoter-luciferase fusion plasmids with or without FOXF2 overexpression plasmid, and the luciferase activity was detected at 48 h post-transfection. (B) The combination of FOXF2 to MSI2 promoter was evaluated by chromatin immunoprecipitation assay. (C) Reverse transcription-quantitative PCR analysis of MSI2 expression in PC cell lines. (D) MSI2 and NUMB protein level shown by western blot analysis. (E) FOXF2 overexpression plasmid and MSI2 siRNA (siMSI2) or control siRNA (siNC) were co-transfected into AsPC-1 cells. Cell Counting Kit-8 assay was conducted to measure cell proliferation. (F) Cell proliferation was determined by 5-ethynyl-20-deoxyuridine staining. (G-I) Representative images and quantitative results of cell migration and invasion assays. Data are indicated as the mean ± SD of at least three independent experiments (n=3). $^{++}$P<0.01 vs. vector + pGL3-MSI2 promoter; **P<0.01 vs. vector; $^{\#\#}$P<0.01 vs. siNC; $^{\wedge}$P<0.05 and $^{\wedge\wedge}$P<0.01 vs. FOXF2 + siNC. FOXF2, forkhead Box F2; PC, pancreatic cancer; MSI2, Musashi 2; siRNA, small interfering RNA; NC, negative control; BS, binding site.

mechanism between FOXF2 and MSI2. CCK-8 assay and EdU staining revealed that MSI2 silencing reversed the promoting effect of FOXF2 on proliferation of PC cells (Fig. 5E and F). Additionally, MSI2 knockdown weakened the facilitation of FOXF2 to the migration and invasion of PC cells (Fig. 5G-I). These results indicated that FOXF2 can bind to the promoter region of MSI2 and promote proliferation, migration and invasion of PC cells possibly by regulating MSI2.

FOXF2 accelerates tumor formation. A xenograft tumor model of PC was constructed to validate the roles of FOXF2 in the development of tumor *in vivo*. Mice were injected with

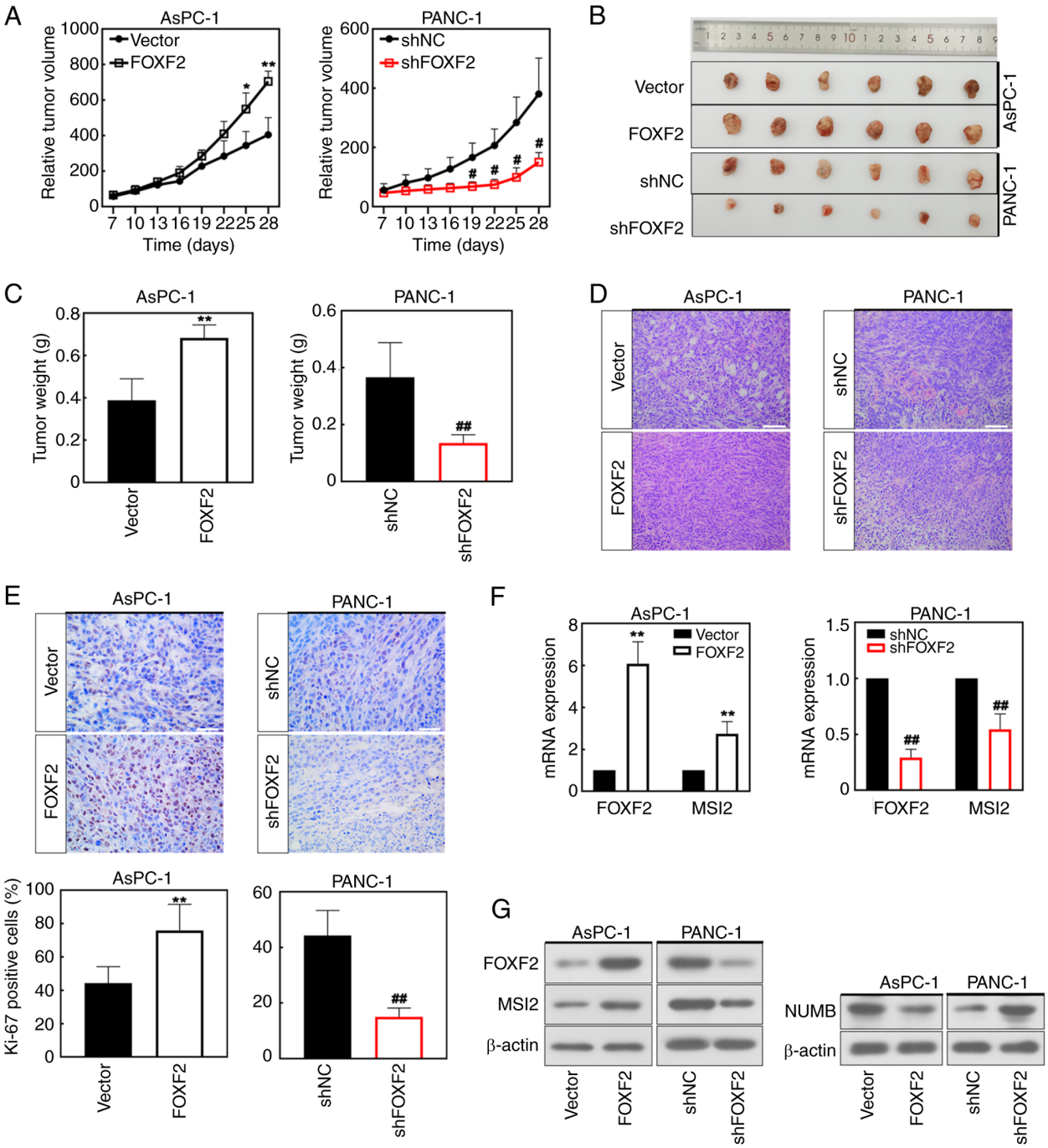

Figure 6. FOXF2 accelerates tumor formation. (A) BALB/c nude mice were subcutaneously injected with the indicated AsPC-1 and PANC-1 cells. The tumor volume was measured every 3 days beginning on day 7 after injection. (B and C) After 28 days, the mice were sacrificed, and tumors were weighed and images were captured. (D) Evaluation of pathological changes in the tumors by H&E staining. (E) Immunohistochemical staining of Ki-67. (F) Relative mRNA expression of FOXF2 and MSI2 detected by reverse transcription-quantitative PCR. (G) Western blot analysis of FOXF2, MSI2 and NUMB. Data are indicated as the mean ± SD of at least six independent experiments (n=6). *P<0.05 and **P<0.01 vs. vector; $^{\#}$P<0.05 and $^{\#\#}$P<0.01 vs. shNC. FOXF2, forkhead Box F2; MSI2, Musashi 2; si-, small interfering; NC, negative control.

the FOXF2-transfected AsPC-1 cells or shFOXF2-transfected PANC-1 cells, respectively. FOXF2 overexpression accelerated the tumor growth while FOXF2 knockdown showed opposite effects (Fig. 6A and B). Results of tumor weight shared the same alteration with those of tumor volume (Fig. 6C). H&E staining demonstrated that FOXF2 maintained the integrity of PC cells and FOXF2 silencing induced the destruction of cell structure (Fig. 6D). In addition, IHC staining indicated that FOXF2 overexpression improved Ki-67 expression (Fig. 6E), suggesting that FOXF2 accelerated the formation of pancreatic tumor *in vivo*. The results of WB and RT-qPCR further revealed that MSI2 expression was significantly increased in the FOXF2-overexpressing mice and decreased in FOXF2-silenced mice (P<0.01) (Fig. 6F). NUMB protein expression showed opposite trends. FOXF2 overexpression downregulated NUMB while FOXF2 knockdown upregulated it in PC tissues (Fig. 6G). Hence, MSI2 could be the target of FOXF2 to promote tumor growth of PC.

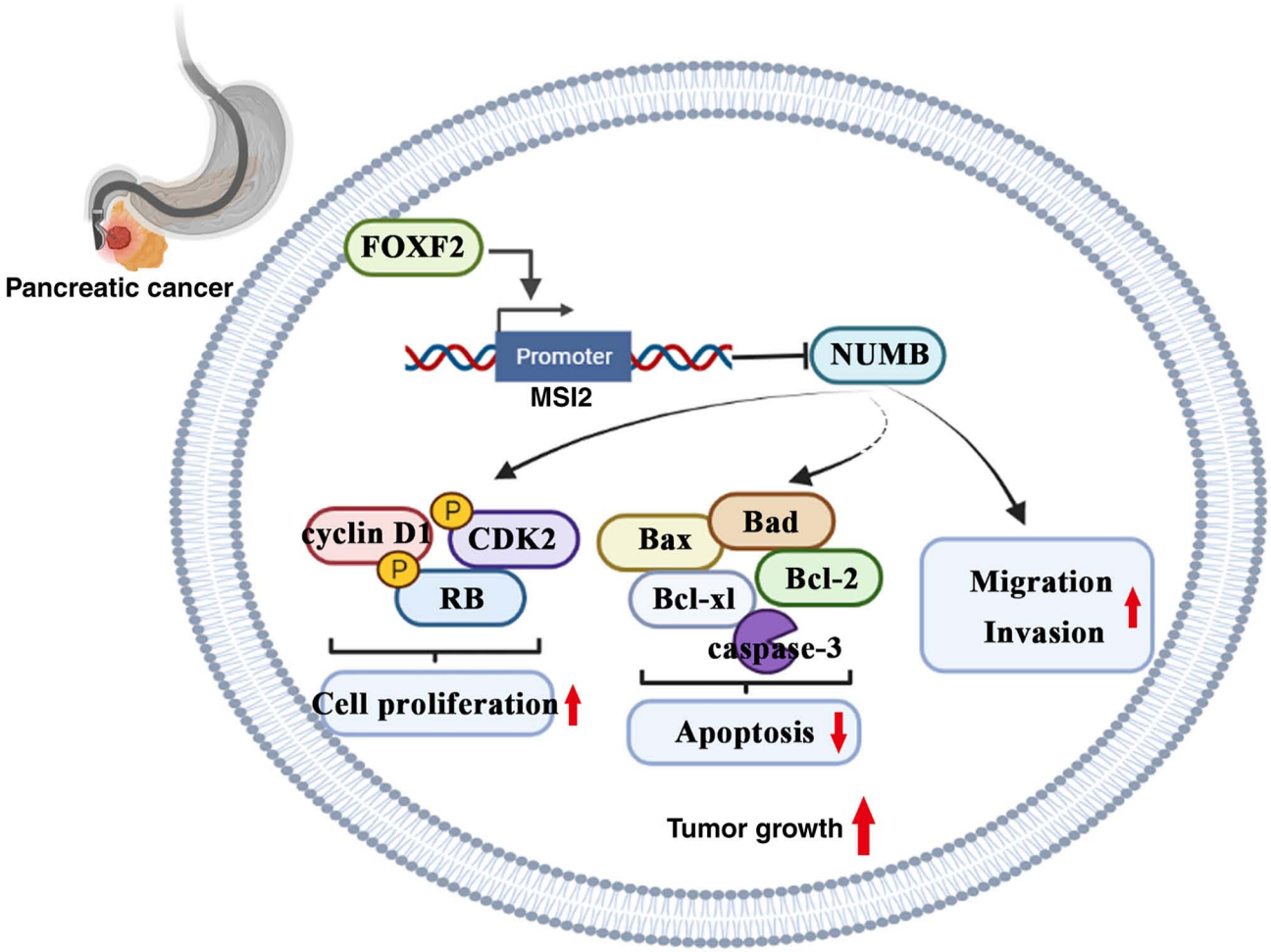

Figure 7. Potential regulatory mechanism of FOXF2 in pancreatic cancer. FOXF2, forkhead Box F2.

Discussion

PC is one of the cancer types with high mortality and featured with insidious onset and atypical early symptoms (23). PC is confused with other digestive diseases, presenting with upper abdominal discomfort, lower back pain, dyspepsia, or diarrhea (24). Current treatments are challenging to benefit all patients because of the inter-individual heterogeneity of PC (4). The average survival is only ~2 years even for patients with PC with surgical resection (25). Therefore, an improved understanding of the molecular mechanisms involved in PC progression is urgently required.

The roles of FOXF2 are well elucidated across various tumors. However, neither the cellular roles nor the regulatory mechanism of FOXF2 in PC has been reported. The current study observed that FOXF2 was highly expressed in PC tissues, particularly in patients with PC at advanced T stage. The present results indicated that high expression of FOXF2 accelerated the proliferation of PC cells *in vitro* and *in vivo*. Similar results were reported in rhabdomyosarcoma cells (12). Additionally, FOXF2 significantly prevented the apoptosis of PC cells. The migration and invasion of PC cells were suppressed by FOXF2 knockdown. Consistently, the promotive effects of FOXF2 on migration and invasion capability were reported in breast cancer cells and lung cancer cells (26,27). On the contrary, FOXF2 inhibited the malignant behavior of colorectal cancer cells (28). FOXF2 suppressed G1-S cell-cycle transition of gastric cancer cell and induced cell apoptosis (22). Therefore, the effect of FOXF2 on tumors depends on the type of cells. The current findings suggested that FOXF2 exerts promotive effects on the growth of PC.

Accumulating evidence elucidated that MSI2 positively regulates the initiation and progression of cancer. Kudinov, Deneka, Nikonova, Beck, Ahn, Liu, Martinez, Schultz, Reynolds, Yang, Cai, Yaghmour, Baker, Egleston, Nicolas, Chikwem, Andrianov, Singh, Borghaei, Serebriiskii, Gibbons, Kurie, Golemis and Boumber (7) reported that MSI2 overexpression enhanced invasion of non-small cell lung cancer cells. MSI2 promoted migration and invasion of PC cells and thus accelerating the progression of PC (4,29). As a transcription factor, FOXF2 involves in the pathogenesis of various tumors through regulating the transcription of downstream genes (30,31). Thus, FOXF2 initiated the transcription of MSI2 in PC cells, and FOXF2 silencing reduced MSI2 expression at transcriptional and translational levels *in vitro* and *in vivo*. Additionally, MSI2 silencing significantly reversed the promotive effects of FOXF2 on proliferation, invasion and migration of PC cells. These findings suggested that MSI2 was the downstream target of FOXF2 in PC. It was previously reported that MSI2 promoted the development and progression

of PC by downregulating NUMB protein (8). The present study also found that FOXF2 knockdown upregulated NUMB at the protein level *in vitro* and *in vivo*. NUMB is a tumor suppressor in several types of tumors (32). The expression of NUMB was downregulated in the esophageal cancer cells, and deficiency of NUMB was associated with poor prognosis and more aggressive tumors in breast and lung cancer (33,34). Collectively, FOXF2 promotes malignant behavior of PC cells possibly through mediating the transcription of MSI2 to downregulate NUMB protein (Fig. 7). Additionally, a previous study by the authors demonstrated that MSI2 promotes invasion and migration of PC cells by upregulating wtp53 protein (9). The ZEB1-ERK/MAPK and ISYNA1-p21/ZEB-1 signaling pathways are involved in the MSI2 regulatory mechanism to facilitate development of PC (4,29). Therefore, FOXF2 could act as an upstream regulator involving in these pathways, which could be explored and verified in further research.

FOXF2 binds to the promoter of MSI2 and promotes its transcriptional expression. The cell migration and invasion are decreased by MSI2 knockdown. Therefore, it was postulated that FOXF2 promoted PC progression possibly via regulating MSI2 transcription. Nevertheless, the upstream regulatory mechanisms of FOXF2 should be elucidated in further researches. In addition to being a target gene of microRNA, FOXF2 is upregulated by specificity protein 1 (SP1), myc-associated zinc-finger protein (MAZ), TGF-β and MCM3AP-AS1 (35-38). Safe, Shrestha, Mohankumar, Howard, Hedrick and Abdelrahim (39) found that SP1 accelerates cell proliferation and migration of PC cells. MAZ is reported to promote invasiveness of PC cells (40). MCM3AP-AS1 promotes cell migration in PC (41). These factors may cause the upregulation of FOXF2 in PC and FOXF2 perhaps mediates their tumor-promoting effect on PC. Further in-depth studies are needed to ascertain the precise molecular regulation of FOXF2 in the development of PC. Besides, an insufficient sample size of clinical specimens limited the exploration of FXOF2 expression and tumor grade. These issues are the current limitations of the present study, and which will be improved in future research.

In summary, FOXF2 promotes proliferation, migration and invasion of PC cells. MSI2 was a transcription regulatory target of FOXF2. FOXF2 accelerates the pancreatic tumor development and progression possibly by regulating an MSI2-NUMB interaction. These findings provide a novel therapy target for PC treatment.

Acknowledgements

Not applicable.

Funding

The present study was supported by the Social Development Program from Shenyang Science and Technology Bureau, China (grant no. F20-205-4-033).

Availability of data and materials

The data generated in the present study are included in the figures and/or tables of this article.

Authors' contributions

MD and YTM contributed to the study conception and design. BHZ, JS and JTT performed material preparation, experiments and analysis. BHZ wrote the first draft of the manuscript and all authors commented on previous versions of the manuscript. All authors read and approved the final manuscript. BHZ and MD confirm the authenticity of all the raw data.

Ethics approval and consent to participate

All animal studies were approved (approval no. KT2021051) by the Laboratory Animal Welfare and Ethics Committee of China Medical University (Shenyang, China). All experiments using human tissue were approved [approval no. (2021) 113] by the Medical Science Research Ethics Committee of The First Affiliated Hospital of China Medical University (Shenyang, China). Written informed consent for the collection of tissue samples was provided by all patients.

Patient consent for publication

Not applicable.

Competing interests

The authors declare that they have no competing interests.

References

1. Vincent A, Herman J, Schulick R, Hruban RH and Goggins M: Pancreatic cancer. Lancet 378: 607-620, 2011.
2. Wood LD, Canto MI, Jaffee EM and Simeone DM: Pancreatic cancer: Pathogenesis, screening, diagnosis, and treatment. Gastroenterology 163: 386-402 e1, 2022.
3. Nakamura M, Okano H, Blendy JA and Montell C: Musashi, a neural RNA-binding protein required for Drosophila adult external sensory organ development. Neuron 13: 67-81, 1994.
4. Sheng W, Shi X, Lin Y, Tang J, Jia C, Cao R, Sun J, Wang G, Zhou L and Dong M: Musashi2 promotes EGF-induced EMT in pancreatic cancer via ZEB1-ERK/MAPK signaling. J Exp Clin Cancer Res 39: 16, 2020.
5. Dong P, Xiong Y, Hanley SJB, Yue J and Watari H: Musashi-2, a novel oncoprotein promoting cervical cancer cell growth and invasion, is negatively regulated by p53-induced miR-143 and miR-107 activation. J Exp Clin Cancer Res 36: 150, 2017.
6. Kharas MG, Lengner CJ, Al-Shahrour F, Bullinger L, Ball B, Zaidi S, Morgan K, Tam W, Paktinat M, Okabe R, *et al*: Musashi-2 regulates normal hematopoiesis and promotes aggressive myeloid leukemia. Nat Med 16: 903-908, 2010.
7. Kudinov AE, Deneka A, Nikonova AS, Beck TN, Ahn YH, Liu X, Martinez CF, Schultz FA, Reynolds S, Yang DH, *et al*: Musashi-2 (MSI2) supports TGF-β signaling and inhibits claudins to promote non-small cell lung cancer (NSCLC) metastasis. Proc Natl Acad Sci USA 113: 6955-6960, 2016.
8. Sheng W, Dong M, Chen C, Li Y, Liu Q and Dong Q: Musashi2 promotes the development and progression of pancreatic cancer by down-regulating Numb protein. Oncotarget 8: 14359-14373, 2017.
9. Sheng W, Dong M, Chen C, Wang Z, Li Y, Wang K, Li Y and Zhou J: Cooperation of Musashi-2, Numb, MDM2, and P53 in drug resistance and malignant biology of pancreatic cancer. FASEB J 31: 2429-2438, 2017.
10. Wang S, Li GX, Tan CC, He R, Kang LJ, Lu JT, Li XQ, Wang QS, Liu PF, Zhai QL and Feng YM: FOXF2 reprograms breast cancer cells into bone metastasis seeds. Nat Commun 10: 2707, 2019.
11. He W, Kang Y, Zhu W, Zhou B, Jiang X, Ren C and Guo W: FOXF2 acts as a crucial molecule in tumours and embryonic development. Cell Death Dis 11: 424, 2020.

12. Milewski D, Pradhan A, Wang X, Cai Y, Le T, Turpin B, Kalinichenko VV and Kalin TV: FoxF1 and FoxF2 transcription factors synergistically promote rhabdomyosarcoma carcinogenesis by repressing transcription of $p21^{Cip1}$ CDK inhibitor. Oncogene 36: 850-862, 2017.
13. Hauptman N, Jevšinek Skok D, Spasovska E, Boštjančič E and Glavač D: Genes CEP55, FOXD3, FOXF2, GNAO1, GRIA4, and KCNA5 as potential diagnostic biomarkers in colorectal cancer. BMC Med Genomics 12: 54, 2019.
14. Zhang J, Zhang C, Sang L, Huang L, Du J and Zhao X: FOXF2 inhibits proliferation, migration, and invasion of Hela cells by regulating Wnt signaling pathway. Biosci Rep 38: BSR20180747, 2018.
15. Wang A, Jin C, Li H, Qin Q and Li L: LncRNA ADAMTS9-AS2 regulates ovarian cancer progression by targeting miR-182-5p/FOXF2 signaling pathway. Int J Biol Macromol 120: 1705-1713, 2018.
16. Lo PK: FOXF2 differentially regulates expression of metabolic genes in non-cancerous and cancerous breast epithelial cells. Trends Diabetes Metab 1: 10.15761/TDM.1000103, 2018.
17. Lo PK, Lee JS, Liang X and Sukumar S: The dual role of FOXF2 in regulation of DNA replication and the epithelial-mesenchymal transition in breast cancer progression. Cell Signal 28: 1502-1519, 2016.
18. Pei H, Li L, Fridley BL, Jenkins GD, Kalari KR, Lingle W, Petersen G, Lou Z and Wang L: FKBP51 affects cancer cell response to chemotherapy by negatively regulating Akt. Cancer Cell 16: 259-266, 2009.
19. Livak KJ and Schmittgen TD: Analysis of relative gene expression data using real-time quantitative PCR and the 2(-Delta Delta C(T)) method. Methods 25: 402-408, 2001.
20. Xia G, Wang H, Song Z, Meng Q, Huang X and Huang X: Gambogic acid sensitizes gemcitabine efficacy in pancreatic cancer by reducing the expression of ribonucleotide reductase subunit-M2 (RRM2). J Exp Clin Cancer Res 36: 107, 2017.
21. Zhou Q and Gallo JM: Differential effect of sunitinib on the distribution of temozolomide in an orthotopic glioma model. Neuro Oncol 11: 301-310, 2009.
22. Higashimori A, Dong Y, Zhang Y, Kang W, Nakatsu G, Ng SSM, Arakawa T, Sung JJY, Chan FKL and Yu J: Forkhead Box F2 suppresses gastric cancer through a novel FOXF2-IRF2BPL-β-catenin signaling axis. Cancer Res 78: 1643-1656, 2018.
23. Torphy RJ, Fujiwara Y and Schulick RD: Pancreatic cancer treatment: Better, but a long way to go. Surg Today 50: 1117-1125, 2020.
24. Zhu H, Wei M, Xu J, Hua J, Liang C, Meng Q, Zhang Y, Liu J, Zhang B, Yu X and Shi S: PARP inhibitors in pancreatic cancer: Molecular mechanisms and clinical applications. Mol Cancer 19: 49, 2020.
25. Heinrich S and Lang H: Neoadjuvant therapy of pancreatic cancer: Definitions and benefits. Int J Mol Sci 18: 1622, 2017.
26. Zhang T, Wan JG, Liu JB and Deng M: MiR-200c inhibits metastasis of breast tumor via the downregulation of Foxf2. Genet Mol Res 16: gmr16038971, 2017.
27. Kundu ST, Byers LA, Peng DH, Roybal JD, Diao L, Wang J, Tong P, Creighton CJ and Gibbons DL: The miR-200 family and the miR-183~96~182 cluster target Foxf2 to inhibit invasion and metastasis in lung cancers. Oncogene 35: 173-186, 2016.
28. Chen J, Ding J, Wang Z, Zhu J, Wang X and Du J: Identification of downstream metastasis-associated target genes regulated by LSD1 in colon cancer cells. Oncotarget 8: 19609-19630, 2017.
29. Zhou L, Sheng W, Jia C, Shi X, Cao R, Wang G, Lin Y, Zhu F, Dong Q and Dong M: Musashi2 promotes the progression of pancreatic cancer through a novel ISYNA1-p21/ZEB-1 pathway. J Cell Mol Med 24: 10560-10572, 2020.
30. Li T, Huang S, Yan W, Zhang Y and Guo Q: FOXF2 regulates PRUNE2 transcription in the pathogenesis of colorectal cancer. Technol Cancer Res Treat 21: 15330338221118717, 2022.
31. Lu JT, Tan CC, Wu XR, He R, Zhang X, Wang QS, Li XQ, Zhang R and Feng YM: FOXF2 deficiency accelerates the visceral metastasis of basal-like breast cancer by unrestrictedly increasing TGF-β and miR-182-5p. Cell Death Differ 27: 2973-2987, 2020.
32. Choi HY, Seok J, Kang GH, Lim KM and Cho SG: The role of NUMB/NUMB isoforms in cancer stem cells. BMB Rep 54: 335-343, 2021.
33. Colaluca IN, Tosoni D, Nuciforo P, Senic-Matuglia F, Galimberti V, Viale G, Pece S and Di Fiore PP: NUMB controls p53 tumour suppressor activity. Nature 451: 76-80, 2008.
34. Pece S, Serresi M, Santolini E, Capra M, Hulleman E, Galimberti V, Zurrida S, Maisonneuve P, Viale G and Di Fiore PP: Loss of negative regulation by Numb over Notch is relevant to human breast carcinogenesis. J Cell Biol 167: 215-221, 2004.
35. Tian HP, Lun SM, Huang HJ, He R, Kong PZ, Wang QS, Li XQ and Feng YM: DNA methylation affects the SP1-regulated transcription of FOXF2 in breast cancer cells. J Biol Chem 290: 19173-19183, 2015.
36. Yu ZH, Lun SM, He R, Tian HP, Huang HJ, Wang QS, Li XQ and Feng YM: Dual function of MAZ mediated by FOXF2 in basal-like breast cancer: Promotion of proliferation and suppression of progression. Cancer Lett 402: 142-152, 2017.
37. Meyer-Schaller N, Heck C, Tiede S, Yilmaz M and Christofori G: Foxf2 plays a dual role during transforming growth factor beta-induced epithelial to mesenchymal transition by promoting apoptosis yet enabling cell junction dissolution and migration. Breast Cancer Res 20: 118, 2018.
38. Dai W, Zeng W and Lee D: lncRNA MCM3AP-AS1 inhibits the progression of colorectal cancer via the miR-19a-3p/FOXF2 axis. J Gene Med 23: e3306, 2021.
39. Safe S, Shrestha R, Mohankumar K, Howard M, Hedrick E and Abdelrahim M: Transcription factors specificity protein and nuclear receptor 4A1 in pancreatic cancer. World J Gastroenterol 27: 6387-6398, 2021.
40. Maity G, Haque I, Ghosh A, Dhar G, Gupta V, Sarkar S, Azeem I, McGregor D, Choudhary A, Campbell DR, *et al*: The MAZ transcription factor is a downstream target of the oncoprotein Cyr61/CCN1 and promotes pancreatic cancer cell invasion via CRAF-ERK signaling. J Biol Chem 293: 4334-4349, 2018.
41. Yu X, Zheng Q, Zhang Q, Zhang S, He Y and Guo W: MCM3AP-AS1: An indispensable cancer-related LncRNA. Front Cell Dev Biol 9: 752718, 2021.